New Maximum Power Point Tracker for PV Arrays Using Fuzzy Controller in Close Cooperation With Fuzzy Cognitive Networks

Theodoros L. Kottas, *Student Member, IEEE*, Yiannis S. Boutalis, *Member, IEEE*, and Athanassios D. Karlis, *Member, IEEE*

***Abstract*—The studies on the photovoltaic (PV) generation are extensively increasing, since it is considered as an essentially inexhaustible and broadly available energy resource. However, the output power induced in the photovoltaic modules depends on solar radiation and temperature of the solar cells. Therefore, to maximize the efficiency of the renewable energy system, it is necessary to track the maximum power point of the PV array. In this paper, a maximum power point tracker using fuzzy set theory is presented to improve energy conversion efficiency. A new method is proposed, by using a fuzzy cognitive network, which is in close cooperation with the presented fuzzy controller. The new method gives a very good maximum power operation of any PV array under different conditions such as changing insolation and temperature. The simulation studies show the effectiveness of the proposed algorithm.**

***Index Terms*—Fuzzy cognitive maps (FCMs), fuzzy cognitive networks (FCN), fuzzy controller, maximum power point tracker (MPPT), photovoltaic systems.**

I. Introduction

WITHOUT a doubt renewable energy systems present unique opportunities for greater fuel diversity, security, and geographical dispersion of supply. The rapid pace of the technical and commercial development of renewable energies continues to reduce costs and increase the number of both equipment suppliers and plant operators. As conventional fossil-fuel energy sources diminish and the world's environmental concern about acid deposition and global warming increases, renewable energy sources (solar, wind, tidal, and geothermal, etc.) are attracting more attention as alternative energy sources. Among the renewable energy sources solar photovoltaic (PV) energy has been widely utilized in small-sized applications. It is also the most promising candidate for research and development for large-scale uses as the fabrication of less-costly photovoltaic devices becomes a reality.

Applications of PV systems include water pumping, domestic and street lighting, electric vehicles, hybrid systems, military and space applications, refrigeration and vaccine storage, power plants, etc., all in either stand-alone or grid-connected configurations. A PV array is by nature a nonlinear power source, which under constant uniform irradiance has a current–voltage (I–V) characteristic like that shown in Fig. 1.

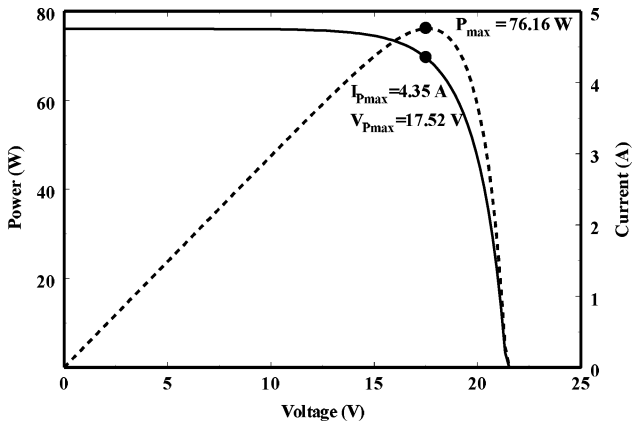

Fig. 1. PV array (I–V) and P–V characteristics.

There is a unique point on the curve, called the maximum power point (MPP), at which the array operates with maximum efficiency and produces maximum output power. As it is well known, the MPP of a PV power generation system depends on array temperature, solar insolation, shading conditions, and PV cells aging, so it is necessary to constantly track the MPP of the solar array. A switch-mode power converter, called a maximum power point tracker (MPPT), can be used to maintain the PV array's operating point at the MPP. The MPPT does this by controlling the PV array's voltage or current independently of those of the load. If properly controlled by an MPPT algorithm, the MPPT can locate and track the MPP of the PV array. However, the location of the MPP in the I–V plane is not known *a priori*. It must be located, either through model calculations or by a search algorithm. Fig. 2 shows a family of PV I–V curves under increasing irradiance, but at constant temperature. Needless to say there is a change in the array voltage at which the MPP occurs. For years, research has focused on various MPP control algorithms to draw the maximum power of the solar array. These techniques include look-up table methods, using neural networks [1], [2], perturbation and observation (P&O) methods [3]–[6], and computational methods [7]. For example, Hiyama *et al*. [1] presented a neural network application to the identification of the optimal operating point of PV modules and designed a PI-type controller for real-time maximum power tracking. Optimal operating voltages are identified through the proposed neural network by using the open-circuit voltages measured from monitoring cells and optimal operating currents are calculated from the measured short-circuit currents.

Manuscript received December 21, 2005. Paper no. TEC-00447-2005.

The authors are with the Department of Electrical and Computer Engineering, Democritus University of Thrace, Xanthi 67100, Greece (e-mail: tkottas@ee.duth.gr; ybout@ee.duth.gr; akarlis@ee.duth.gr).

Digital Object Identifier 10.1109/TEC.2006.875430

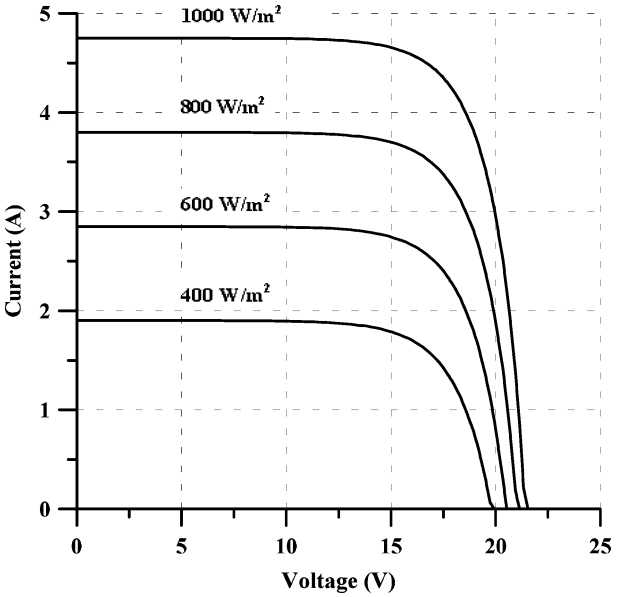

Fig. 2. PV array (I–V) characteristics at various insolation levels.

The output of the neural network goes through the PI controller to the voltage control loop of the inverter to change the terminal voltage of the PV system to the identified optimal one.

One of the computational methods, which have demonstrated fine performances under different environmental operating conditions, is the fuzzy-based MPPT technique [8], [9].

The fuzzy controller introduced in [8] uses dP/dI and its variations $\Delta(dP/dI)$, as the inputs and computes MPPT converter duty cycle. The fuzzy tracker of [9] considers variation of duty cycle, but replaces dP/dI by the variation of panel power. An on-line search algorithm that does not require the measurement of temperature and solar irradiation level is proposed in reference [10]. Other researchers analyzed and compared the various MPPT techniques [7], [11], [12]. Besides that, in [11] a simple DSP-based MPPT algorithm is proposed, while in [12] a combination of the modified constant voltage control and the incremental conductance method is introduced, showing good efficiency (especially in lower insolation intensity). Finally, in [13], [14] efforts have been made to model the dynamic behavior of a PV system in order to study its interaction with the pertinent MPPT system, while in [15], MPPT assessment and testing methods were presented in order to identify the accuracy, error and efficiency of the MPPTs.

This paper presents a novel MPPT method, which uses fuzzy sets theory [8] in close cooperation with fuzzy cognitive networks (FCNs). FCNs [16], [17] constitute an extension of the well-known fuzzy cognitive maps (FCMs) [18], so that they are able to operate in continuous interaction with the physical system they represent, while at the same time they keep track of the various operational equilibrium points met by the system. FCNs can model dynamical complex systems that change with time following nonlinear laws. They use a symbolic representation for the description and modeling of the system. In order to illustrate different aspects in the behavior of the system, an FCN is consisted of nodes with each node representing a characteristic

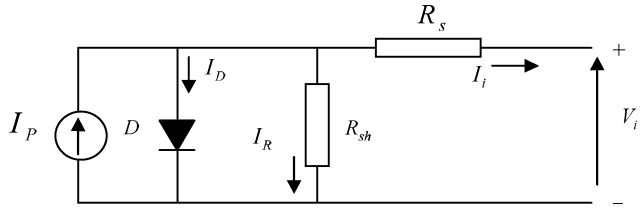

Fig. 3. Equivalent circuit of a solar cell.

of the system, including possible control actions. These nodes interact with each other showing the dynamics of the system under study. Moreover, the FCN has the ability of continuous interaction with the physical system it represents, sending control actions and receiving feedback from the system. The FCN integrates the accumulated experience and knowledge on the operation of the system, as a result of the method by which it is constructed, i.e., using human experts who know the operation of system and its behavior, but most significantly, it can adapt this knowledge based on the feedback from the physical system or by using appropriate training data.

In this paper, an FCN is presented and a novel control system is designed so that fuzzy controller [8] can cooperate with FCN, in order to solve the MPPT problem of a PV system. The nodes of the FCN represent essential operational (Voltage, Current, Insolation, Temperature) and control (Current) variables of the PV system. The node interconnection weights are determined using data, which are constructed so that they cover the operation of a PV system under a wide range of different climatic conditions. Once the FCN is trained it can be mounted on any PV system. Moreover, during the operation of the PV array the FCN weights are continuously updated based on data from the encountered operating conditions. The performance of the method is tested using climatic data for a specific PV system of the market, which reaches its MPP with great accuracy for various operational conditions, such as changing insolation and temperature and seasonal variations.

The paper is organized as follows. In Section II, mathematical relations between the essential variables of a PV system are presented. These relations are necessary for simulating its operation under different insolation and temperature levels. In Section III, an MPPT method, which is based on a fuzzy controller methodology is analyzed. Section IV makes a brief introduction in FCMs and presents the graph of the proposed FCN, which will be used in close cooperation with the fuzzy controller, in order to track the MPP of a PV system. Simulated experimental results, based on climatic data of one year and on the operation of a typical PV array of the market are given in Section V. Finally, Section VI concludes the work.

II. Simulation of the PV System

Using the equivalent circuit of a solar cell (Fig. 3) and the pertinent equations [11] the nonlinear (I–V) characteristics of a solar array are extracted, neglecting the series resistance

$$I_i = I_{\rm ph} - I_{\rm rs}\exp[(qV_i/kTA) - 1] - \frac{V_i}{R_{\rm sh}} \qquad (1)$$

TABLE I
FACTOR A DEPENDENCE ON PV TECHNOLOGY

Technology	A
Si-mono	1.2
Si-poly	1.3
a-Si:H	1.8
a-Si:H tandem	3.3
a-Si:H triple	5
CdTe	1.5
CIS	1.5
AsGa	1.3

where I_i is the PV array output current (A); V_i is the PV array output voltage (V); q is the charge of an electron; k is Boltzmann's constant in J/K; A is the p–n junction ideality factor; T is the cell temperature (K); and $I_{\rm rs}$ is the cell reverse saturation current. The factor A in (1) determines the cell deviation from the ideal p–n junction characteristics. The ideal value ranges between 1 and 5, according to [11] and to the commercially available software package for PV systems PVSYST V3.1 (see Table I).

The photocurrent $I_{\rm ph}$ depends on the solar radiation and the cell temperature as stated in the following:

$$I_{\rm ph} = (I_{\rm scr} + k_i(T - T_r))\frac{s}{100}, \tag{2}$$

where $I_{\rm scr}$ is the PV array short circuit current at reference temperature and radiation (A); k_i is the short circuit current temperaturecoefficient (A/K) and S is the solar radiation (mW/cm^2).

The reverse saturation current $I_{\rm rs}$ varies with temperature, according to the following:

$$I_{\rm rs} = I_{\rm rr}\left(\frac{T}{T_{\rm r}}\right)^3 \exp\left[\frac{1.115}{k'A}\left(\frac{1}{T_{\rm r}} - \frac{1}{T}\right)\right] \tag{3}$$

where $T_{\rm r}$ is the cell reference temperature, $I_{\rm rr}$ is the reverse saturation current at $T_{\rm r}$, $k\prime$ is the Boltzmann's constant in eV/K and the bandgap energy of the semiconductor used in the cell is equal to 1.115.

Finally, the next equation was used in the computer simulations to obtain the open circuit voltage of the PV array

$$V_{\rm oc} = \frac{AkT}{q}\ln\left(\frac{I_{\rm ph} + I_{\rm rs}}{I_{\rm rs}}\right). \tag{4}$$

From (2) to (4), we get

$$I_{\rm rr} = \frac{(I_{\rm scr} + k_i(T - T_{\rm r}))\frac{s}{100}}{\exp[(V_{\rm oc}q/AkT) - 1]} \times \left(\left(\frac{T_{\rm r}}{T}\right)^3 \exp\left[-\frac{1.115}{k'A}\left(\frac{1}{T_{\rm r}} - \frac{1}{T}\right)\right]\right) \tag{5}$$

and from (1)

$$R_{\rm sh} = \frac{V_{\rm oc}}{-I_{\rm rs}(\exp[(qV_{\rm oc}/kTA) - 1]}. \tag{6}$$

The required data for identifying the maximum operating point at any insolation level and temperature are the following:

1) k_i;
2) open circuit voltage $V_{\rm oc}$ (for initial conditions $T_{\rm r} = 25\,^\circ$C, $S = 100$ mW/cm^2);
3) short circuit current $I_{\rm scr}$ (for initial conditions $T_{\rm r} = 25\,^\circ$C, $S = 100$ mW/cm^2);
4) maximum power voltage $V_{\rm mp}$ (for initial conditions $T_{\rm r} = 25\,^\circ$C, $S = 100$ mW/cm^2);
5) maximum power current $I_{\rm mp}$ (for initial conditions $T_{\rm r} = 25\,^\circ$C, $S = 100$ mW/cm^2) all given by the PV array manufacturer.

III. MPPT BY FUZZY LOGIC CONTROLLER [8]

The control objective is to track and extract maximum power from the PV arrays for a given solar insolation level. The maximum power corresponding to the optimum operating point is determined for a different solar insolation level. Normally a dc–dc converter is utilized between the input source and the load for the purpose of MPPT.

A. Fuzzification

In [8], the authors focused on single input–single output plant, in which control is determined on the basis of satisfaction of two criteria relating to two input variables of the presented controller, namely error (E) and change of error (CE), at a sampling instant k.

The variable E and *CE* are expressed as follows:

$$E(k) = \frac{P_{\rm pv}(k) - P_{\rm pv}(k-1)}{I_{\rm pv}(k) - I_{\rm pv}(k-1)} \tag{7}$$

$$\mathrm{CE}(k) = E(k) - E(k-1) \tag{8}$$

where $P_{\rm pv}(k)$ and $I_{\rm pv}(k)$ are the power and current of the PV array, respectively. Therefore, $E(k)$ is zero at the maximum power point of a PV array. In Fig. 4(a), the fuzzy set of input $E(k)$ is presented, while in Fig. 4(b), the fuzzy set of input $\mathrm{CE}(k)$ is shown. Finally, Fig. 4(c) shows the respective fuzzy set of the output dD, which represents the change of the on/off duty ratio of the switch S of a stepup boost converter similar to the one shown in Fig. 5.

B. Inference Method

Table II shows the rule table of the fuzzy controller where all the entries of the matrix are fuzzy sets of error $E(k)$ change of error $\mathrm{CE}(k)$, and change of duty ratio dD to the boost converter. In the case of fuzzy control, the control rule must be designed in order that input variable $E(k)$ has to always be zero.

As an example control rule in Table II:

IF E is *PB* AND *CE* is *ZO* THEN dD is *PB*

As a fuzzy inference method, Mamdani's method is used with max–min operation fuzzy combination law. For the defuzzification the center of area (COA) and the max criterion method (MCM) is used [19].

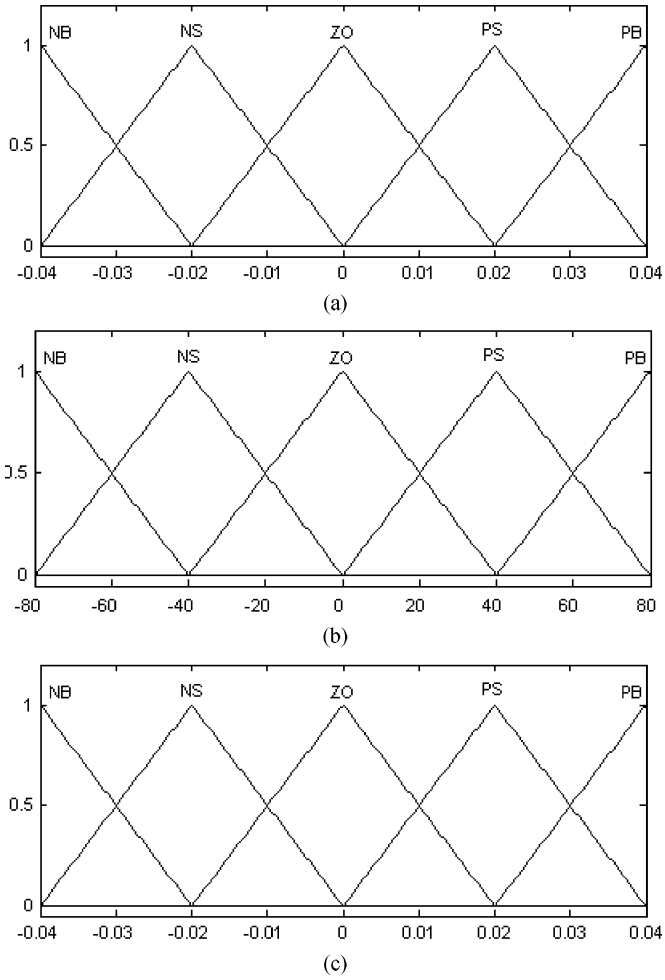

Fig. 4. Membership function for (a) input $E(k)$; (b) input $CE(k)$; (c) output dD.

TABLE II
FUZZY RULE TABLE

CE / E	NB	NS	ZO	PS	PB
NB	ZO	ZO	NB	NB	NB
NS	ZO	ZO	NS	NS	NS
ZO	NS	ZO	ZO	ZO	PS
PS	PS	PS	PS	ZO	ZO
PB	PB	PB	PB	ZO	ZO

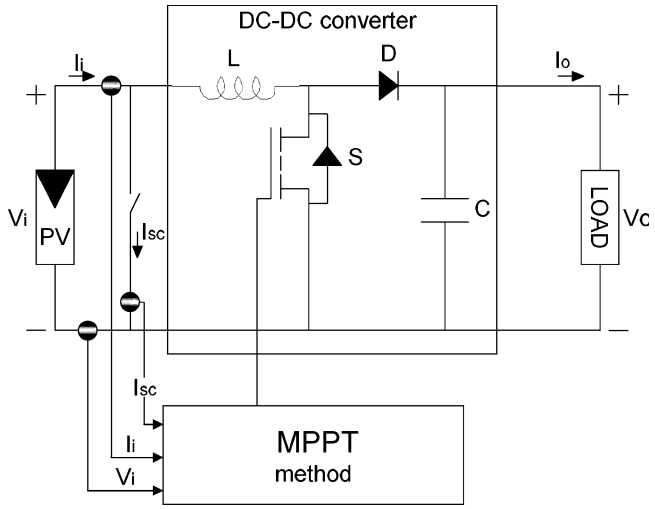

Fig. 5. Stepup boost converter for MPPT.

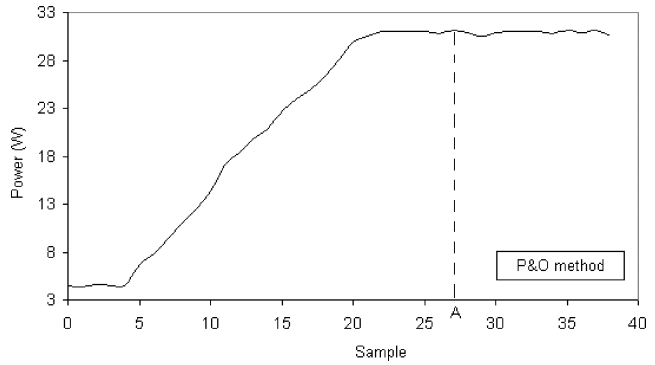

Fig. 6. Sample versus power of PV array using P&O method. At point A, the P&O method reaches the MPP for first time after iteration (27).

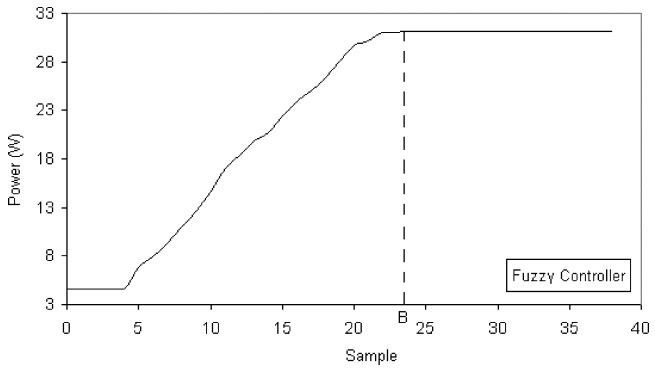

Fig. 7. Sample versus power of PV array, using fuzzy controller method. At point B, the fuzzy controller's method reaches MPP after iteration (24).

The characteristics of the simulated dc–dc boost converter are given in the Appendix A.

We choose to use the fuzzy controller method as MPPT instead of the simple P&O method [20], because by doing so there is a reduction not only in the time required to track the MPP but also in the fluctuation of power, as it is clearly presented in Figs. 6 and 7.

So far the fuzzy controller is performing better compared to the classic P&O one by adjusting appropriately the voltage of the dc–dc converter, in order to reach the MPP of a PV array, faster and with no fluctuation. Some disadvantages of the fuzzy controller's method are eliminated using FCN. As it is well known, the MPP of a PV array varies according to temperature and/or insolation variations; thus, the fuzzy controller starts its search for this new MPP, by using as starting point the previous MPP (corresponding to the previous temperature and insolation

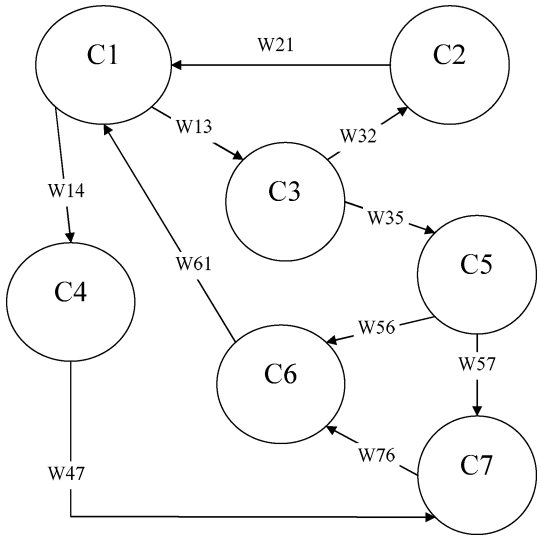

Fig. 8. Simple fuzzy cognitive map.

levels). This devolvement demands a considerable number of iterations, especially if this new MPP is located far away from the previous one, which means that the wasted energy is significant. A faster devolvement from one MPP to another is ensured with the use of an FCN, just like the proposed one presented in the next section. It will be shown in the following results that FCN, in close cooperation with the presented fuzzy controller, will become a robust MPPT method, in order to minimize the wasted energy.

IV. FCN Approach for the Photovoltaic Project

In this section, we will present an FCN designed to represent the operation of a photovoltaic system. Our aim is to use the FCNs, which are extensions of FCMs, for estimating the maximum power point of the photovoltaic system.

A. FCMs

FCMs approach is a hybrid modeling methodology, exploiting characteristics of both fuzzy logic and neural networks theories, and it may play an important role in the development of intelligent manufacturing systems. The utilization of existing knowledge and experience on the operation of complex systems is the core of this modeling approach.

The graphical illustration of an FCM is a signed directed graph with feedback, consisting of nodes and weighted interconnections. Nodes of the graph stand for the nodes that are used to describe the behavior of the system and they are connected by signed and weighted arcs representing the causal relationships that exist among nodes (Fig. 8).

Each node represents a characteristic of the system. In general it stands for states, variables, events, actions, goals, values, trends of the system, which is modeled as an FCM [18]. Each node is characterized by a number A_j, which represents its value and it results from the transformation of the real value of the system's variable, for which this node stands, in the interval [0, 1]. It must be mentioned that all the values in the graph are fuzzy, and so weights of the interconnections belong to the interval $[-1, 1]$. With the graphical representation of the behavioral model of the system, it becomes clear which node of the system influences other nodes and in which degree. The weight of the interconnection between node C_i and node C_j denoted by W_{ij}, could be positive ($W_{ij}>0$) for positive causality or negative ($W_{ij}<0$) for negative causality or there is no relationship between node C_i, and node C_j, thus $W_{ij} = 0$.

The causal knowledge of the dynamic behavior of the system is stored in the structure of the map and in the interconnections that summarize the correlation between cause and effect. The value of each node is influenced by the values of the connected nodes with the corresponding causal weights and by its previous value. So, the value A_j for each node C_j is calculated by the following rule [21]:

$$A_j^s = f\left(\sum_{i=1, i\neq j}^{N} A_i^{s-1} W_{ij} + A_j^{s-1}\right) \tag{9}$$

where A_j^s, is the value of node C_j at step s, A_i^{s-1} is the value of node C_i, at step $s-1$, A_j^{s-1} is the value of node C_j at step $s-1$, and W_{ij} is the weight of the interconnection between nodes C_i and C_j · f is a squashing function: $f = 1/[1+\mathrm{e}^{-cx}]$. By using $c = 1$, we convert the nodes values in the range [0,1].

To account for the existence of steady nodes, (9) has to be slightly modified so that it does not provide with erroneous results. Steady value nodes are the nodes that influence the remaining graph but they are not influenced by any other node of the graph. In this case, nodes values are now computed through equations [16]

$$A_j^{s,\mathrm{FCM}} = f\left(\sum_{i=1, i\neq j}^{N} A_i^{s-1,\mathrm{FCM}} W_{ij} + A_j^{s-1,\mathrm{FCM}}\right). \tag{10}$$

And for the steady-state nodes the correction equation is

$$A_j^{s,\mathrm{FCM}} = A_j^{\mathrm{system}} \tag{11}$$

where A_j^{system} is the node's value, derived from the physical system.

B. Cognitive Graph for the PV Project

The graph shown in Fig. 9 represents a photovoltaic system, for a MPPT use. The graph have six nodes, where nodes C1, C2, and C6 are steady value nodes and nodes C3, C4, C5 could be control nodes. In this approach, node C4 is the control node whose value is used to regulate the current of the system. The regulation of the current of the system means that a different power is now the output power of the photovoltaic. Control nodes are the nodes the values of which will be used to the real system as control actions. Node C4 is used to calculate the optimum current needed to regulate the output power of the photovoltaic in the maximum point. The nodes of the graph

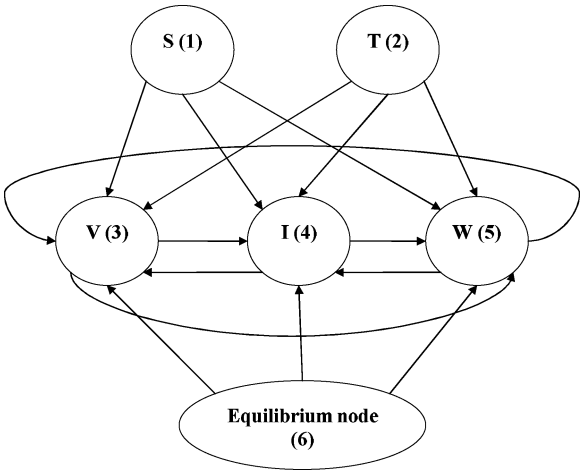

Fig. 9. FCN designed for the photovoltaic project.

are related to the following physical quantities of the photovoltaic system.

Node C1 represents the irradiation with range in the interval [0, 1], 0 is the minimum point of the irradiation (usually 0 mW/cm^2) and one is the maximum point, corresponding to 100 mW/cm^2.

Node C2 represents the temperature that also must be in the interval [0, 1]. Zero is the minimum point of the temperature (usually $-30\,^{\circ}$C) and one is the maximum point, usually $70\,^{\circ}$C.

Node C3 represents the optimum voltage of the photovoltaic system for the climatologic data obtained at the specific point of time, which also must be in the interval [0, 1], 0 is the minimum point of the voltage (usually 0 V) and one is the maximum point $V_{\max}$, where $V_{\max}$ is calculated, according to (4) by setting $T = T_{\min}$ and $S = S_{\max}$.

Node C4 represents the optimum current of the photovoltaic system for the climatologic data obtained at the specific point of time, which also must be in the interval [0, 1]. Here 0 is the minimum point of the current (usually 0 A) and 1 is the maximum point $I_{\max}$, where $I_{\max}$ is calculated, according to (2) by setting $T = T_{\max}$ and $S = S_{\max}$.

Node C5 expresses the optimum output power of the photovoltaic system for the climatologic data obtained at the specific point of time, which also must be in the interval [0, 1]. Here 0 is the minimum point of the power (usually 0 W) and 1 is the maximum point $W_{\max}$, where $W_{\max}$ is a characteristic given from PV operational data under $T_{\min}$ and $S_{\max}$.

Node C6 is an artificial design node, the value of which is used to regulate the equilibrium point in the nodes C3, C4, and C5. The value of C6 is steady and equals 1. The weights W_{63}, W_{64}, and W_{65}, respectively, are originally set to 0 and are allowed to change only, when one or more weights affecting nodes 3, 4, and 5 exceed the value of absolute 1. For example the value of weight W_{63} is allowed to be updated when the weights that affect node C3 (W_{13}, W_{43}, and W_{53}) are going to take values larger from the absolute value 1. In this situation, weight is activated and its value is no longer set to zero. By using equilibrium node C6 and the weights connecting this node with nodes C3, C4, and C5, we manage to regulate the values of nodes C3, C4, and C5, by always keeping values of the graph weights below absolute value 1.

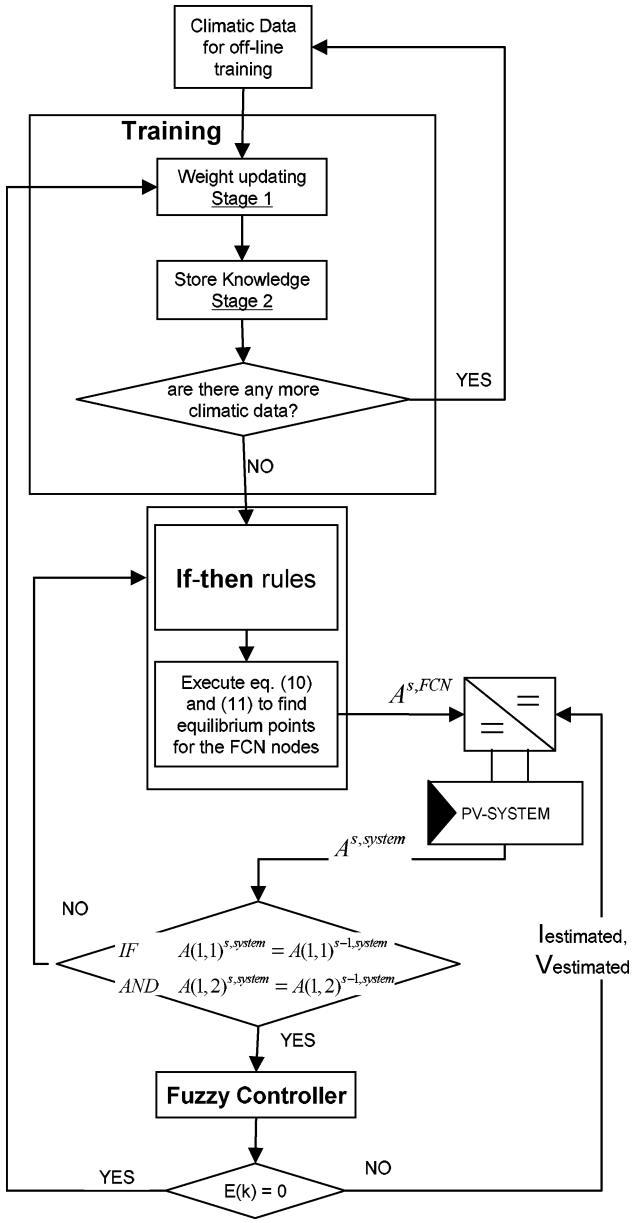

Fig. 10. Simplified flowchart of the proposed method.

C. FCN Approach for the Photovoltaic Project

FCN [16], [17], constitute an extension of FCMs. Unlike FCMs, which rely only on the use of the initially acquired experts' knowledge about the operation of the system and which is represented by the weights values of the map, FCNs may use these values only as a starting point or may not use them at all. The operation of FCNs is tightly connected with the operation of the physical system providing control values and taking feedback from the system. Moreover, during its initial training or its subsequent interaction with the physical system, the FCN keeps track of its previous equilibrium points by means of a collection of fuzzy if–then rules. Using these characteristics, the FCN

becomes a dynamic control system. In this paper we use the FCN in close cooperation with a fuzzy MPPT controller and with a PV system as shown in Fig. 10. The FCN is first off-line trained by appropriately constructed data and then it is connected to any PV system to get feedback and send control values to regulate its output. Once the FCN is trained its knowledge can be updated and the FCN acts as an adaptive controller of the PV system. The off-line training and the subsequent operation are described bellow.

1) Initial Off-Line Training of the FCN: The off-line training is being performed in an incremental manner. This means that for each training data vector that contains PV value variables corresponding to different operation conditions, the FCN weights are updated to comply with the data vector. Moreover, this new acquired knowledge is been stored in a fuzzy-rule data base. We can divide the training into two cooperating stages.

2) Stage 1—Weight Updating Using New Data: This stage is concerned with the method of updating the interconnections weights of FCN taking into account training data. Since the training is being performed incrementally, during stage 1, only one data vector is used. The FCN converges to its new weights values after a number of iterations. In each training iteration the FCN uses the updated weights to reach new equilibrium node values by means of (10) and (11). These values are compared to the given training values and the error is given for the new updating iteration. The weight updating is used by the following extended delta rule [16]

$$p = A_j^{\text{system}} - \frac{1}{1+e^{-\left(\sum_{i=1,i\neq j}^{N} A_i^{\text{system}} W_{ij} + A_j^{\text{system}}\right)}} = A_j^{\text{system}} - A_j^{\text{FCN}} \quad (12)$$

$$W_{ij}^{k} = W_{ij}^{k-1} + R_{ij} * (ap(1-p))A_i^{\text{FCN}} \quad (13)$$

where p is the error, k is the number of iteration, a is the learning rate (usually $a = 0.1$) and R_{ij} is a calibration variable, which prevents the FCN node and weight values from being driven in their saturation point. R_{ij} can be computed by the following [16]:

$$R_{ij} = \eta \frac{\sum_{i=1}^{i=n} |W_{ij}|}{|W_{ij}|} \quad \text{if } W_{ij} \neq 0 \quad \text{and} \quad R_{ij} = 0 \text{ if } W_{ij} = 0 \quad (14)$$

where constant value η is used to drive values R_{ij} in the range [0, 1]. In most practical situations, $\eta = 0.1$.

3) Stage 2–Storage of the New Knowledge in a Fuzzy Rule Database: The procedure described in the previous stage modifies our knowledge about the system by continuously modifying the weight interconnections and consequently, the node values. After the weight updating is taking place, the FCN reaches a new equilibrium point using (10) and (11). Since a new training vector might produce different weights and different equilibrium point we have to keep track of the current knowledge (weights and equilibrium points) to be used after the training

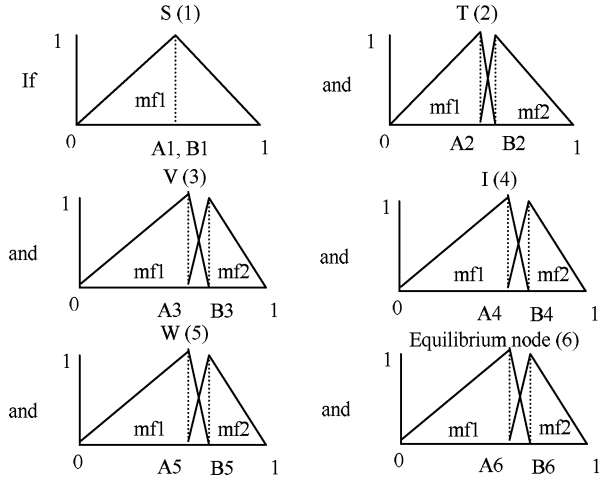

Fig. 11. Left-hand side ("if" part).

phase. We do that by producing fuzzy if–then rules, according to the following procedure [17].

Suppose, for example, that the FCN after being trained by a data vector converges to the following weight matrix:

$$W = \begin{bmatrix} 0 & 0 & W13 & W14 & W15 & 0 \\ 0 & 0 & W23 & W24 & W25 & 0 \\ 0 & 0 & 0 & W34 & W35 & 0 \\ 0 & 0 & W43 & 0 & W45 & 0 \\ 0 & 0 & W53 & W54 & 0 & 0 \\ 0 & 0 & W63 & W64 & W65 & 0 \end{bmatrix}$$

and concludes to an equilibrium point, which is

$$A = [A1 \quad A2 \quad A3 \quad A4 \quad A5 \quad A6].$$

Suppose also that for a new training data vector, it concludes to a new equilibrium point

$$B = [B1 \quad B2 \quad B3 \quad B4 \quad B5 \quad B6]$$

with weight matrix

$$K = \begin{bmatrix} 0 & 0 & K13 & K14 & K15 & 0 \\ 0 & 0 & K23 & K24 & K25 & 0 \\ 0 & 0 & 0 & K34 & K35 & 0 \\ 0 & 0 & K43 & 0 & K45 & 0 \\ 0 & 0 & K53 & K54 & 0 & 0 \\ 0 & 0 & K63 & K64 & K65 & 0 \end{bmatrix}.$$

The fuzzy rule database, which is obtained using the information from the two previous equilibrium points, is depicted in Figs. 11 and 12 and is resolved as follows:

There are two rules related to the above two different equilibrium situations

Rule 1

if node 1 is mf1 and node 2 is mf1 and node 3 is mf1 and node 4 is mf1 and node 5 is mf1 and node 6 is mf1

then w13 is mf1 and w14 is mf1 and w15 is mf1 and w23 is mf1 and w24 is mf1 and w25 is mf1 and w34 is mf1 and w35 is mf1 and w43 is mf1 and w45 is mf1 and w53 is mf1 and w54 is mf1 and w63 is mf1 and w64 is mf1 and w65 is mf1

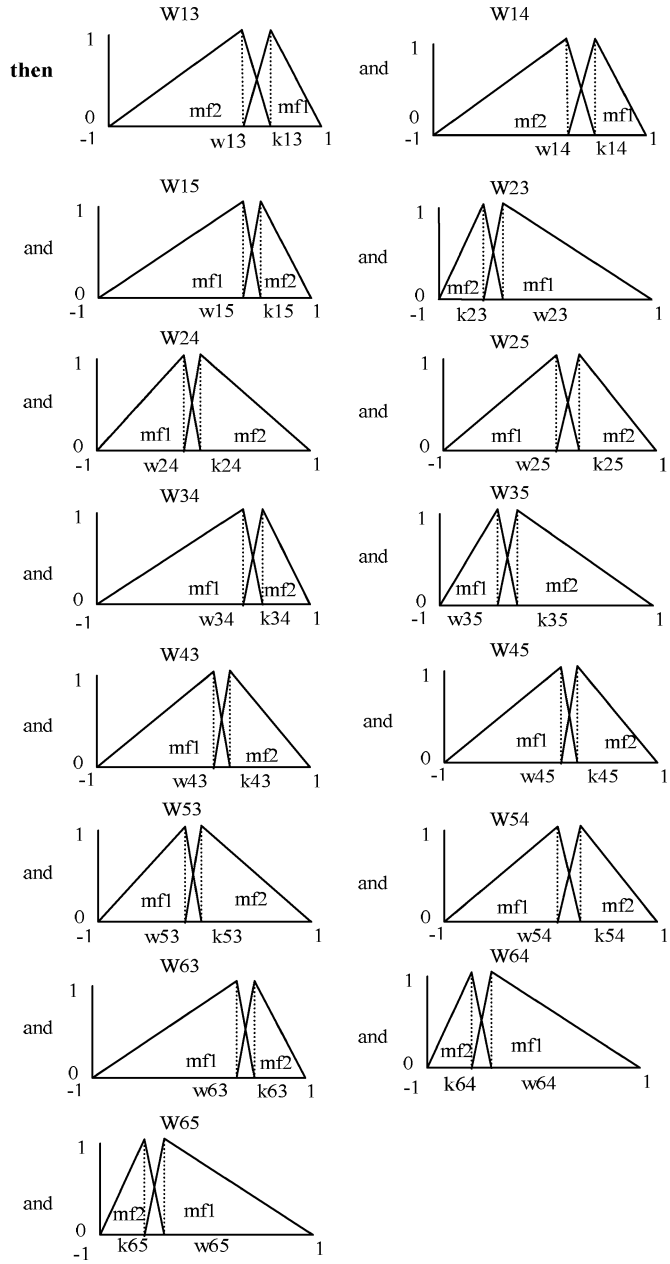

Fig. 12. Right-hand side ("then" part).

Rule 2
if node 1 is mf1 and node 2 is mf2 and node 3 is mf2 and node 4 is mf2 and node 5 is mf2 and node 6 is mf2
then w13 is mf2 and w14 is mf2 and w15 is mf2 and w23 is mf2 and w24 is mf2 and w25 is mf2 and w34 is mf2 and w35 is mf2 and w43 is mf2 and w45 is mf2 and w53 is mf2 and w54 is mf2 and w63 is mf2 and w64 is mf2 and w65 is mf2.

The number and shape of the fuzzy membership functions of the variables of both sides of the rules are gradually modified as new desired equilibrium points appear to the system during its training. To add a new triangular membership function in the fuzzy description of a variable, the new value of the variable must differ from one already encountered value more than a specified threshold. The threshold comes usually as a compromise between the maximum number of allowable rules and the detail in fuzzy representation of each variable.

Once the new knowledge has been stored using the above procedure we run again stage 1 using a new training vector. The procedure stops after all data vectors have been presented.

4) Control of a PV System Using the Trained FCN and the Fuzzy Controller: Once the FCN is off-line trained, it can be connected to the PV system according to Fig. 10. The FCN receives feedback from the fuzzy controller and from the PV array also. Once the error $E(k)$ of the fuzzy controller is set to zero, it means that the duty ratio of the switch S of the boost converter is set to the proper value, so that the PV array is in its maximum power point. This new maximum power point gives a new equilibrium point to the FCN. The new equilibrium point is used to train further the FCN. If there is a change in the values of temperature and insolation before the fuzzy controller drives the duty ratio of the switch S to the proper value corresponding to the MPP then the FCN interferes to the procedure and sends a new proper value for MPP voltage for the new insolation and temperature.

V. Results

Needless to say that irradiation and temperature play the most significant role on the maximum power that is drawn from a PV module. In order to measure these two quantities a pyranometer and a thermocouple is often used, although the output from these two measuring devices is not always the most adequate information to identify the operating point yielding the maximum power, which is of course a drawback of this methodology. The short circuit current from the PV array gives the most adequate information of the effective insolation and temperature using (1)–(6).

We construct training data for the FCN using the following procedure: We use some typical climatic data. These data are chosen to be Irradiation (S-node 1). We select values in the range 0–100 mW/cm^2 using a step of 5 mW/cm^2. Temperature (T-node 2). We select values in the range $-30\,^{\circ}$C–$70\,^{\circ}$C, using a step of $5\,^{\circ}$C.

By using all the possible combinations of these data and by using the simulation of the photovoltaic array, we calculate the values of the optimum voltage (node 3), current (node 4), and output power (node 5) from (1) to (4). Using these node values for nodes 1–5, we update the weights of the FCN according to stage 1 of the training procedure and for the equilibrium point derived for any possible combination, we store the knowledge according to stage 2.

The possible combinations of the climatic data are 441 and the FCN creates 21 triangular fuzzy numbers for nodes 1 and 2, 24 for node 3, 48 for node 4, 43 for node 5, 5 for node 6. Also, 287 fuzzy if–then rules are created to store the knowledge. The number of rules appears to be large because they account for all possible combinations of climatic data, even for those which are unlikely ever to occur. This number could be significantly reduced if we exclude this kind of combinations.

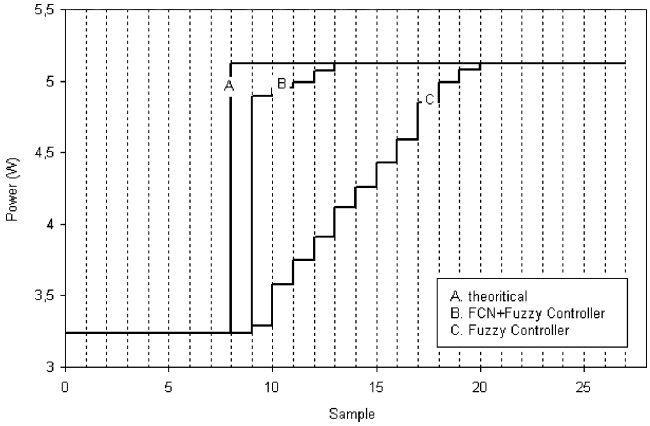

Fig. 13. Sample versus power of PV-array. (A) Theoretical, (B) proposed method, and (C) fuzzy controller.

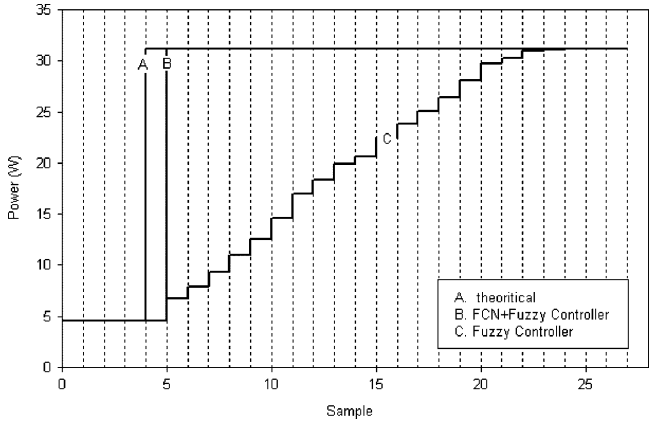

Fig. 14. Sample versus power of PV-array. (A) Theoretical, (B) proposed method, and (C) fuzzy controller.

When we connect the FCN system to the PV array, if the error $E(k)$ is zero, fuzzy MPPT controller sends the values of nodes 1 and 2 to the training part of the algorithm and through the fuzzy rule database, the system decides, which weights values are appropriate to express the values of nodes 3, 4, and 5. Executing (10) and (11) and by using the weights derived above, we calculate the new equilibrium point which expresses the values of the optimum current, voltage and output power of the PV array for the climatic data obtained at the specific time instant. In the next step the FCN sends the values of the control nodes to the dc–dc boost converter, thus determining the optimum current, which corresponds to the maximum output power for the climatic data obtained at the specific time instant.

In order to evaluate the effectiveness of the proposed algorithm, we used the trained FCN for controlling the operation of the BP270L PV array. The parameters of the PV array are given in Appendix B, where a sample of the weight matrix and the corresponding equilibrium points is also given. Fig. 13 presents a comparison between (A) the theoretical (computed by (1)–(4)) MPP, (B) the calculated by the proposed FCN and fuzzy controller method and (C) the calculated by only the fuzzy controller method [8]. It is clearly depicted that by using the FCN + fuzzy controller MPPT system, we have a significant energy gain. Actually, the combined method needs only five iterations, in order to reach the new MPP, while the fuzzy controller method alone needs 12 iterations, in order to reach the same MPP. Each iteration corresponds to one second, following the same sampling procedure with [8].

In Fig. 14, a similar comparison among the performance of the three methods but in different temperature and insolation conditions than those of Fig. 13 is given. We can see that the new MPP was exactly the point that the FCN instantly returned to the dc–dc converter for the new insolation and temperature levels. That is why the proposed method (B) does not need to use the fuzzy controller, in order to reach the MPP. In this case by using the proposed method we reach the MPP after only one iteration, while by using only the fuzzy controller the system reached the MPP after 18 iterations.

Fig. 15 amply demonstrates the reason why it is better to use off-line training. As we can see the system is in an MPP, corresponding to a specific insolation and temperature level. The next MPP, corresponding to another insolation and temperature level, is a point with which the FCN has already been trained off-line. Using, as feedback from the PV array, the values of current, voltage and sort circuit current and by using (1)–(4) the control system calculates the insolation and the temperature corresponding to the feedback values. The so computed insolation and temperature values are in this case values with which FCN has already been trained off-line. Thus, the proposed method returns the optimum control law instantly to the dc–dc converter, as it is shown in Fig. 15 (plot B). If there was no off-line training, then the values of insolation and temperature, corresponding to the new MPP, would not be values for insolation and temperature, with which the FCN has already been trained. In this case the FCN returns initially an MPP value, which is far away from the actual one. Therefore, the proposed method will need a number of steps before reaching the actual MPP (plot D). It has to be mentioned that this phenomenon appears mainly in the beginning of the operation of the method, when the FCN is totally untrained. After a sufficient time of operation the FCN gains experience and therefore it acts as if it was initially off-line trained.

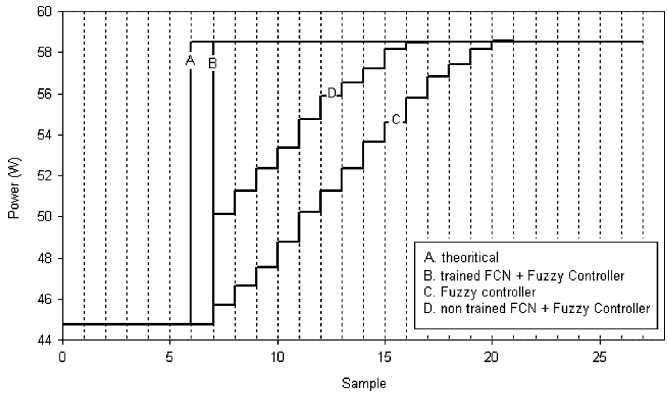

Fig. 15. Sample versus power of PV-array. (A) Theoretical, (B) proposed method (off-line trained FCN), (C) fuzzy controller, and (D) proposed method (only on-line trained FCN).

TABLE III
COMPARISON OF VARIOUS MPPT METHODS

MPPT Method	kWh (P_X)	error (%) $(P_A-P_X)/P_A$
A. Theoretical total energy within year 2002	P_A=70.389	
B. Off-line trained FCN + Fuzzy Controller	P_B=70.38745	0.78
C. Fuzzy Controller	P_C=65.96857	6.28
D. Only on-line trained FCN + Fuzzy Controller	P_D=68.995	1.98

Finally, in order to estimate the energy gain of the new method (FCN + fuzzy controller MPPT) in comparison to the method which uses fuzzy controller only we performed the following experiment. Using data from the year 2002 we ran both methods to give us the maximum power points and calculated the energy acquired from the PV array. Both methods are compared to the optimal one [theoretical MPP values, computed by using (1)–(4)] and the results are shown in Table III. It can be observed that the proposed method (both cases B and D) outperforms method C (fuzzy controller only). Actually, when the off-line trained FCN is used the proposed method provides with only a 0.78% less energy production than the optimal (theoretical) case.

A typical real life application of the proposed methodology would require the following steps.

1) Once a specific PV array is selected its parameters, as those indicated in Appendix B, are entered to the controller.
2) Based on these parameters the training data are produced using the various combinations of the climatic data and (1)–(4).
3) The FCN is being off-line trained using the above data and according to the procedure described in Section IV.
4) Once the FCN is off-line trained, it is left to operate with the specific PV array in close cooperation with the fuzzy controller.

It is evident that this procedure can be applied to any PV array of the market.

VI. CONCLUSION

A novel method for maximum power point tracking was presented in this paper. The method combines a fuzzy MPPT with an appropriately designed FCN to speed-up the procedure of reaching the accurate maximum power point of a photovoltaic array under changing environmental conditions. The method presents very good results, i.e., only 0.78% error in energy production when compared with the theoretical expected production of a commercially available photovoltaic array, simulated on climatic data of a whole year. The methodology can be applied on any photovoltaic array of the market. Due to the existence of the FCN the method could track and adapt to any physical variations of the photovoltaic array through time. Therefore, the method is guaranteed to present its very good performance independently of these variations.

APPENDIX A

The dc–dc boost converter has been simulated, according to characteristics described below:

1) Array: BP270L PV array;
2) dc–dc converter input voltage $(V_{\rm i})$: 13.7–24.7 V;
3) dc–dc converter output voltage $(V_{\rm o})$: 48 V;
4) Switching frequency (fs): 33 kHz.

Below are shown the basic equations necessary for the dc–dc boost converter design [22]

$$\frac{V_{\rm o}}{V_{\rm i}} = \frac{1}{1-D}, \frac{I_{\rm i}}{I_{\rm o}} = \frac{1}{1-D}, \text{ where } D = \frac{t_{\rm on}}{T} \text{ and } T = \frac{1}{fs}.$$

APPENDIX B

PV system data:

i) $k_i = 2.8$ mA/°C;
ii) Open circuit voltage $V_{\rm oc} = 21.4$ V;
iii) Short circuit current $I_{\rm scr} = 4.48$ A;
iv) Maximum power voltage $V_{\rm mp} = 17.1$ V;
v) Maximum power current $I_{\rm mp} = 4.15$ A.

Based on the node description presented in Section IV and by using the PV system data given by the manufacturer we can see, as an example, an equilibrium point with weight matrix

$$W = \begin{bmatrix} 0 & 0 & -0.0013 & -0.5962 & -0.387 & 0 \\ 0 & 0 & -0.0462 & -0.7528 & -0.4822 & 0 \\ 0 & 0 & 0 & -0.4097 & -0.4695 & 0 \\ 0 & 0 & -0.3731 & 0 & -0.632 & 0 \\ 0 & 0 & 0.0347 & 0.4454 & 0 & 0 \\ 0 & 0 & 0 & -0.7392 & -0.869 & 0 \end{bmatrix}$$

and $\boldsymbol{A}$ vector is

$$\boldsymbol{A} = [0.247 \quad 0.5762 \quad 0.6288 \quad 0.2179 \quad 0.1837 \quad 1].$$

The $\boldsymbol{A}$ vector means that

$$S = 24.7 \text{ mW/cm}^2, \quad T = 27.62\,^{\circ}\text{C}, \quad V = 16 \text{ V},$$
$$I = 1.003 \text{ A}, \quad W = 16.048 \text{ W}.$$

REFERENCES

[1] T. Hiyama, S. Kouzuma, and T. Imakubo, "Identification of optimal operating point of PV modules using neural network for real time maximum power tracking control," *IEEE Trans. Energy Convers.*, vol. 10, no. 2, pp. 360–367, Jun. 1995.
[2] K. Ro and S. Rahman, "Two-loop controller for maximizing performance of a grid-connected photovoltaic-fuel cell hybrid power plant," *IEEE Trans. Energy Convers.*, vol. 13, no. 3, pp. 276–281, Sep. 1998.
[3] M. Miyatake, T. Kouno, and M. Nakano, "A simple maximum power tracking control employing fibonacci search algorithm for power conditioners of photovoltaic generators," presented at the 10th Int. EPE-PEMC, Cavtat and Dubrovnik, Croatia, 2002.
[4] A. B. G. Bahgat, N. H. Helwa, G. E. Ahmad, and E. T. El Shenawy, "Maximum power point tracking controller for PV systems using neural networks," *Renew. Energy*, vol. 30, pp. 1257–1268, 2005.
[5] Z. Salameh and D. Taylor, "Stepup maximum power point tracker for photovoltaic arrays," *Solar Energy*, vol. 44, pp. 57–61, 1990.
[6] E. Koutroulis, K. Kalaitzakis, and N. C. Voulgaris, "Development of a microcontroller-based, photovoltaic maximum power point tracking control system," *IEEE Trans. Power Electron.*, vol. 16, no. 1, pp. 46–54, Jan. 2001.
[7] M. A. S. Masoum, H. Dehbonei, and E. F. Fuchs, "Theoretical and experimental analyses of photovoltaic systems with voltage- and current-based maximum power-point tracking," *IEEE Trans. Energy Convers.*, vol. 17, no. 4, pp. 514–522, Dec. 2002.

[8] C.-Y. Won, D.-H. Kim, S.-C. Kim, W.-S. Kim, and H.-S. Kim, "A new maximum power point tracker of photovoltaic arrays using fuzzy controller," in *25th Annu. IEEE PESC* Jun. 20–25, 1994, vol. 1, pp. 396–403.
[9] M. G. Simoes and N. N. Franceschetti, "Fuzzy optimization based control of a solar array," *Proc. IEE Electr. Power Appl.*, vol. 146, no. 5, pp. 552–558, Sep. 1999.
[10] I. H. Altas and A. M. Sharaf, "A novel on-line MPP search algorithm for PV arrays," *IEEE Trans. Energy Convers.*, vol. 11, no. 4, pp. 748–754, Dec. 1996.
[11] C. Hua and C. Shen, "Study of maximum power tracking techniques and control of dc–dc converters for photovoltaic power system," in *Proc. 29th Annu. IEEE PESC* May 17–22, 1998, vol. 1, pp. 86–93.
[12] G. J. Yu, Y. S. Jung, J. Y. Choi, and G. S. Kim, "A novel two-mode MPPT control algorithm based on comparative study of existing algorithms," *Solar Energy*, vol. 76, pp. 455–463, 2004.
[13] H. Matsukawa, K. Koshiishi, H. Koizumi, K. Kurokawa, M. Hamada, and L. Bo, "Dynamic evaluation of maximum power point tracking operation with PV array simulator," *Solar Energy Mater. Solar Cells*, vol. 75, pp. 537–546, 2003.
[14] M. A. S. Masoum, S. M. M. Badejani, and E. F. Fuchs, "Microprocessor-controlled new class of optimal battery chargers for photovoltaic applications," *IEEE Trans. Energy Convers.*, vol. 19, no. 3, pp. 599–606, Sep. 2004.
[15] M. Jantsch *et al.*, "Measurement of PV maximum power point tracking performance," presented at the 14th Eur. Photovoltaic Solar Energy Conf. and Exhibition, Barcelona, Spain, Jun. 30–Jul. 4 1997.
[16] T. Kottas, Y. Boutalis, and M. Christodoulou, "A new method for weight updating in Fuzzy cognitive maps using system feedback," in *Proc. 2nd ICINCO*, Barcelona, Spain, Sep. 13–17, 2005, pp. 202–209.
[17] Y. Boutalis, T. Kottas, B. Mertzios, and M. Christodoulou, "A Fuzzy rule based approach for storing the knowledge acquired from dynamical FCMs," in *Proc. 5th ICTA*, Thessalonica, Greece, Oct. 15–16, 2005, pp. 119–124.
[18] B. Kosko, "Fuzzy cognitive Maps," *Int. J. Man-Mach. Stud.*, pp. 65–75, Jan. 1986.
[19] C. Lee, "Fuzzy logic in control systems: Part I and part II," *IEEE Trans. Syst., Man, Cybern.*, vol. 20, no. 2, pp. 404–435, Mar.–Apr. 1990.
[20] C. Hua and C. Shen, "Comparative study of peak power tracking technics for solar storage system," in *Proc. 13th Annu. Appl. Power Electr. Conf. Expo.*, 1998, vol. 2, pp. 679–685.
[21] C. Stylios and P. Groumpos, "Fuzzy cognitive maps: A model for intelligent supervisory control systems," *Comput. Ind.*, vol. 39, pp. 229–238, 1999.
[22] J. Santos and F. Antunes, "Maximum power point tracker for PV systems," in *Proc. World Climatic Energy Event*, Rio de Janeiro, Brazil, 2003, pp. 75–80.

Theodoros L. Kottas (S'06) received the Dipl.Eng. and M.Sc. degrees in electrical and computer engineering from Department, Democritus University of Thrace, Xanthi, Greece, in 2003 and 2005, respectively. He is currently working toward the Ph.D. degree at the Automatic Control Systems Laboratory, Department of Electrical and Computer Engineering, Democritus University of Thrace.

His research interests include intelligent modeling and control techniques with applications in power production and conversion.

Mr. Kottas is a member of the Technical Chamber of Greece.

Yiannis S. Boutalis (M'86) received the diploma in electrical engineering from the Democritus University of Thrace, Xanthi, Greece, in 1983, and the Ph.D. degree in electrical and computer engineering from the Computer Science Division of National Technical University of Athens, Athens, Greece, in 1988.

He served as an Assistant Visiting Professor at the University of Thessaly, Greece, and as a Visiting Professor at the Air Defense Academy of General Staff of Air Forces of Greece. He also served as a Researcher at the Institute of Language and Speech Processing (ILSP), Greece, and as a Managing Director of the R&D SME Ideatech S.A, Greece, specializing in pattern recognition and signal processing applications. Since 1996, he has been a Faculty Member, at the Department of Electrical and Computer Engineering, Democritus University of Thrace, where he is currently working as an Associate Professor. His current research interests include the development of computational intelligence techniques with applications in control, pattern recognition, signal and image processing problems.

Athanassios D. Karlis (M'00) received the diploma in electrical engineering and the Ph.D. degree in electrical and computer engineering from the Electrical and Computer Engineering Department, Aristotle University of Thessaloniki, Thessaloniki, Greece, in 1991 and 1996, respectively.

Currently, he is working as a Lecturer at the Electrical Machines Laboratory, Department of Electrical and Computer Engineering, Democritus University of Thrace, Xanthi, Greece. His research interests include electrical machines, power production from small hydro, wind energy conversion and photovoltaics, power systems, and electrical installations.

Dr. Karlis is a member of the Technical Chamber of Greece.